Supporting information

Tunable Metal-Polyaniline Interface for Efficient Carbon Dioxide Electro-reduction to Formic acid and Methanol in Aqueous Solution

Weiran Zheng,[a,b] Simantini Nayak,[a] Weizi Yuan,[a] Zhiyan Zeng,[c] Xinlin Hong,[c] Kylie A. Vincent,[a] and Shik Chi Edman Tsang [a]*

[a] Department of Chemistry, University of Oxford, Oxford, OX1 3QR, United Kingdom

[b] Department of Applied Biology and Chemical Technology, the Hong Kong Polytechnic University, Hong Kong SAR, P. R. China

[c] College of Chemistry and Molecular Sciences, Wuhan University, Wuhan, 430072, P. R. China

Experimental:

Chemicals: Ammonium peroxidodisulfate (APS), HCl, $NH_3 \cdot H_2O$, aniline, $(NH_4)_2PdCl_4$, $(NH_4)_2PtCl_4$, $CuSO_4$, Sodium borohydride ($NaBH_4$), Dimethylformamide (DMF) and 98% H_2SO_4. All chemicals were purchased from Sigma-Aldrich, and used as received. Distilled water (DI water) was used for the washing. 18.5 MΩ Ultrapure water was used for all electrochemical measurements, and 0.5 M H_2SO_4 aqueous solution was used for electrochemical experiments.

Synthesis of PANI: The synthesis process of PANI nanofiber was described in literature.[1] Aniline (16 mmol) and Ammonium persulfate (APS) (4 mmol) were dispersed in 50 mL 1 M HCl aqueous solution respectively. The two solutions were rapidly mixed together continuingly stirring at 1000 rpm. The mixture was kept in ice bath (0 °C) for 24 h. The colour of the solution changed from light yellow to dark green. After reaction, the solution was filtered using a FluoroporeTM PTFE membrane filters (pore size 200 nm, from Sigma-Aldrich). Green residue was collected. Then, excessive amount of 1 M $NH_3 \cdot H_2O$ aqueous solution was used to wash the green residue until the colour changed to dark blue (de-doping process, from ES form to EB form). The residue was further washed using distilled water (DI water) 5 times until the filtrate turned colourless. The solid was collected and dried in oven at 100 °C overnight.

Synthesis of metal/PANI: For the synthesis of metal/PANI composite, *in situ* reduction process was used. PANI powder (2 mmol of repeating unit, EB form) was dispersed in 25 mL DMF and sonicated for 30 min. Then, $(NH_4)_2PdCl_4$, $(NH_4)_2PtCl_4$ and $CuSO_4$ (0.4 mmol) was added correspondingly to the suspension to prepare metal/PANI (molar ratio of metal/N = 1:5). The suspension was sonicated for another 30 min. $NaBH_4$ solution (1 g/mL in DMF) was introduced at room temperature as reducing agent, molar ratio of $NaBH_4$ to metal ion was 15:1. The solution was stirred (500 rpm) and kept at room temperature for 5 h to ensure fully reduction of metal precursor. The suspension was filtered and residue was washed 5 times with DI water. The solid was collected and dried in oven at 100 °C overnight. *Only the Pd content in PANI was checked by ICP-MS and EDX against the expected recipe value, which showed the total reduction of the Pd precursor into the solid form and no residue Pd was found in the filtrate.*

Characterization methods:

Electron microscopy: Transmission electron microscopy (TEM, JEOL Model JEM-2100F) and Scanning electron microscopy (SEM, JEOL Model JSM-6335F) were used to get the electron microscopy images of samples.

X-ray diffraction (XRD): XRD analysis was carried out on a PANalytical X'Pert Pro diffractometer, the experiment is operated in the Bragg–Brentano focusing geometry and used Cu-K_α radiation (λ = 1.5418 Å) from a generator operating at 40 kV and 40 mA.

Thermogravimetric analysis (TGA): TGA was performed using a Q50 TA thermogravimetric analysis system. The analysis was carried out in air and the heating rate was 5 °C min^{-1}.

Fourier transform infrared spectroscopy (FTIR): FTIR was performed on a NICOLET 6700 instrument from Thermo Scientific. Specac's Golden Gate™ Attenuated total reflectance (ATR) accessory (Diamond crystal) was used with liquid nitrogen cooled MCT detector. IR spectra were collected for 64 scans with a resolution of 2 cm^{-1}.

***In situ* electrochemical Infrared spectroscopy:** For the *in situ* electrochemical IR spectroscopic measurements an Agilent FTIR spectrometer with liquid N_2 cooled MCT detector was used, and spectra were collected at a resolution of 4 cm^{-1}. An Autolab potentiostat (128N) was used to apply electrochemical control. A Si internal reflection element (IRE, Crystal GmbH, Germany) with dimension of 5 * 8 * 1 mm^3 and 39˚ angle of incidence at both the short edges was used. Before every experiment the Si IRE was sonicated with 30 % conc. H_2SO_4 and cleaned with deionized water. It was

mounted on the baseplate of the home made spectroelectrochemical cell fabricated from of polyether ether ketone (PEEK),[2,3] and sealed with silicone glue into baseplate. 5 mg mL^{-1} PANI and Pd/PANI dispersed in ethanol was prepared and 10 μL of solution was drop cast onto the Si IRE and dried in air. A sheet of carbon paper (TGP-H-030, Toray Industries, Inc.) was placed on the dried ink and used to make contact with glassy carbon rod from the top. A Ag/AgCl, (BAS Inc.) electrode was used as reference electrode and Pt wire was used as the counter electrode. The spectroelectrochemical cell was then mounted on a modified ATR accessory (GladiATR, PIKE Technologies). 0.5 M H_2SO_4 solution was saturated either with N_2 or H_2 and flowed into the cell using a peristaltic pump (flow speed: 10 mL min^{-1}).

IR spectra were collected in kinetics mode in every 1 s and co-added, at the simultaneous onset of CV method triggered by the potentiostat. IR spectra recorded at the initial potential were used as reference spectra to calculate difference absorbance spectra at other potentials.

CO_2-temperature programed desorption (CO_2-TPD): TPD was carried out on an AutoChem II 2920 instrument supplied by Micromeritics. The sample was reduced under H_2 at 100 °C first and then cooled down to room temperature in Ar. The CO_2 gas was passed through the sample for 1 h to achieve highest adsorption. Then, He gas was passed through to remove excessive CO_2. The test was run at a heat speed of 10 °C/min. The plots were normalized according to PANI mass.

Gas chromatography-mass spectrometry (GC-MS): GC-MS was done on an Agilent 7890A gas chromatography for detection of HCOOH, CH_3OH and other possible products.

^{1}H-Nuclear magnetic resonance (^{1}H-NMR): ^{1}H-NMR experiment was run on a 400 MHz instrument provided by Bruker.

Liquid chromatography (LC): Agilent 1260 LC system provided by Agilent Technologies for HCOOH and CH_3OH detection. Flow rate is 0.25 mL/min; mobile phase is 0.1 M H_2SO_4 aqueous solution. Detection wavelength is 210.16 nm.

Gas chromatography (GC): Agilent 7890B GC system.

X-ray photoelectron spectroscopy (XPS): XPS was run on an ESCA 3400 X-Ray Photoelectron Spectrometers provided by SHIMADZU.**Raman spectroscopy:** Raman spectrum was acquired on Thermo-Nicolet 6700 FT-Raman Spectrophotometer. Laser wavelength was 632 nm. The energy of laser was set at 5%.

Rotating disk electrode (RDE) preparation: For electrochemical testing of a catalyst, a glassy carbon rotating disk electrode (RDE) electrode was used with the diameter measured to be 7 mm (area 0.385 cm^2). The electrode was carefully polished using aqueous Al_2O_3 slurries (1 μm, 300 nm and 50 nm), and sonicated and washed using deionised water. The PANI and metal/PANI samples were dispersed in DMF and sonicated for 1 h, with the concentration of 5 mg PANI mL^{-1}. Then 10 μL of the sample suspension was dropped on the electrode and the electrode was left to dry at room temperature for 60 mins.

Cyclic voltammetry (CV) and CO_2 electro-reduction: The electrochemical experiments were carried out using an RDE on a VersaSTAT 3 potentiostat provided by AMETEK, Princeton Applied Research. All experiments were done at room temperature using a Ag/AgCl (saturated KCl) reference electrode (0.198 V vs SHE, room temperature) in 0.5 M H_2SO_4 solution. CV experiments were carried out in a one-compartment cell and CO_2 electro-reduction experiments were done in a H-shaped two-compartment cell, the total liquid volume of the cell is 10 mL. Platinum wire in a coiled form was used as counter electrode whose surface area is many times higher compared to our working electrode. The rotation rate of the RDE for CV experiments was set at 500 rpm, and the rotation rate of the RDE for CO_2 electro-reduction was 800 rpm. The scan rates are indicated in the figure captions. For CO_2 electro-reduction, CO_2 gas was bubbled through the solution for 1 h prior to the experiment to reach saturation. The electrode was then kept at a target potential (-0.5 V, -0.7 V, -0.9 V and -1.1 V vs SHE) for 180 min, and CO_2 gas was continuously flowed over the solution during this period. The final solution was collected and used for GC-MS and NMR measurements.

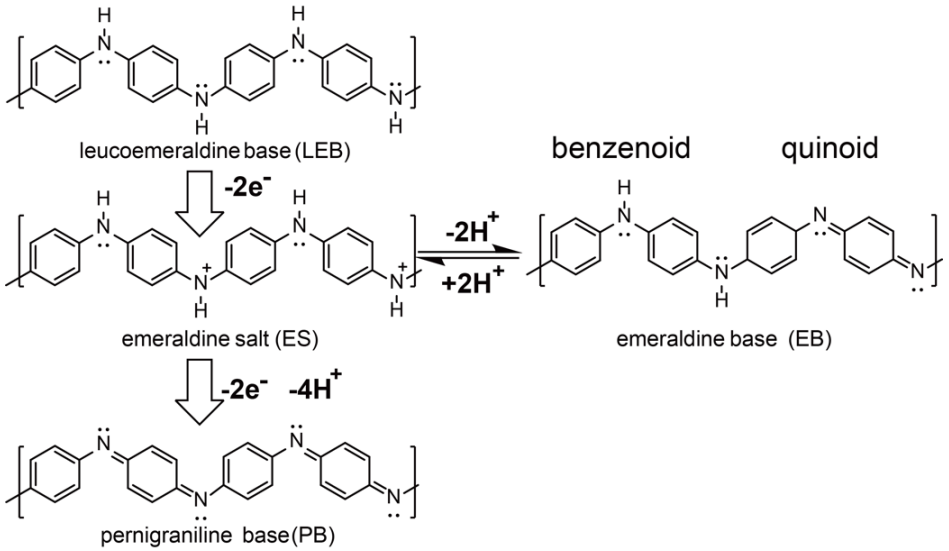

Scheme S1 Redox modes of PANI.

Figures and calculations:

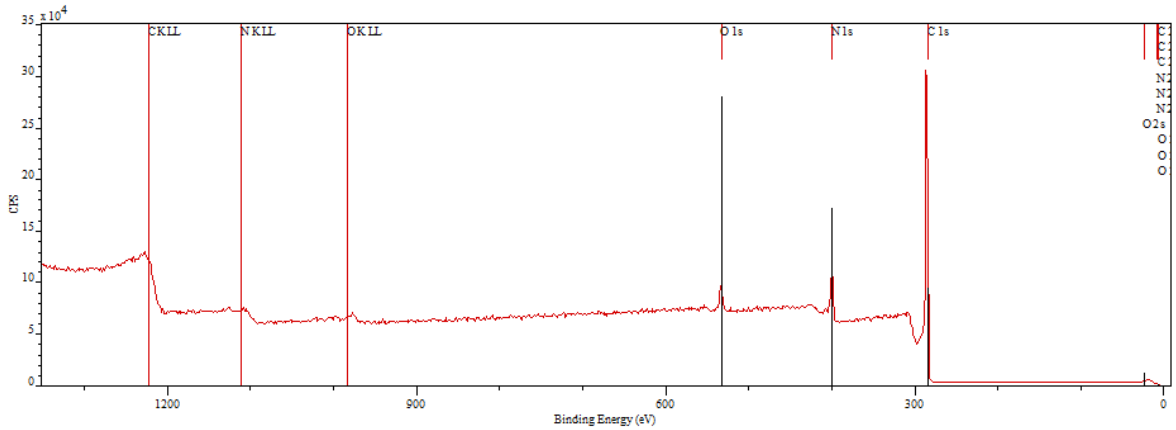

Figure S1 XPS survey of PANI.

As shown in **Figure S1**, the result of XPS survey analysis agreed with the literature report that there is an absence of Cl signal (binding energy of Cl_{2s} locates at 268.79 eV).[4] It means that the PANI has been converted to the EB form from the HCl doped form (emeraldine salt, ES) after treatment.

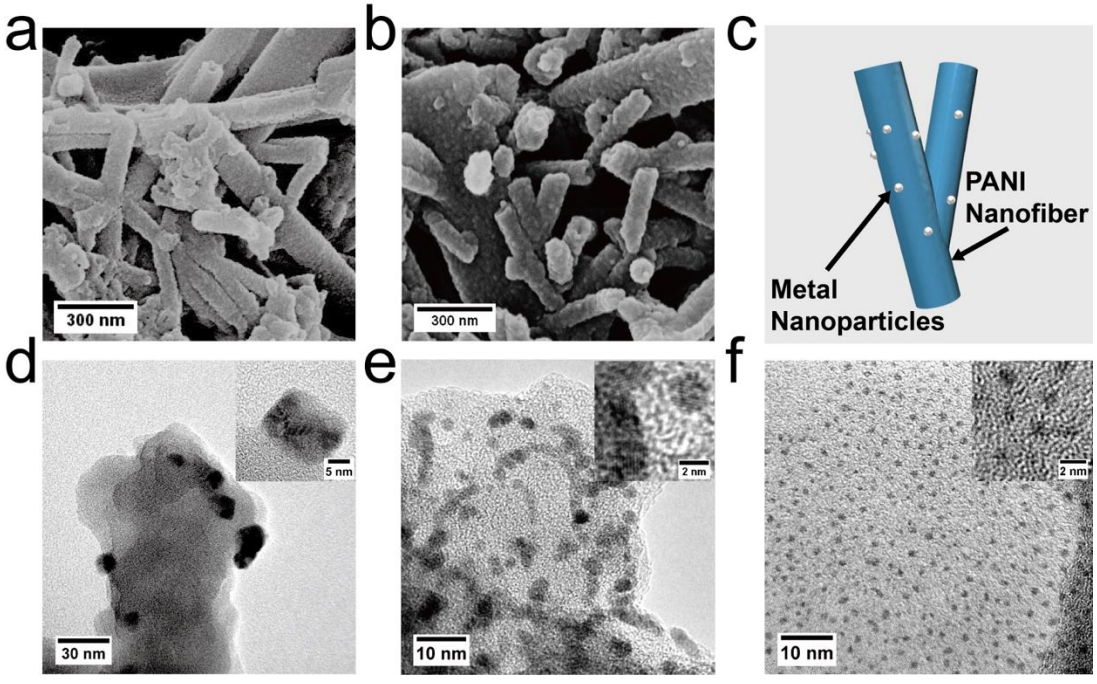

Figure S2 SEM images of (a) PANI and (b) Pd/PANI; (c) An illustration of metal/PANI; TEM images of (d) Cu/PANI, (e) Pd/PANI and (f) Pt/PANI, inserts: selected areas of high magnification.

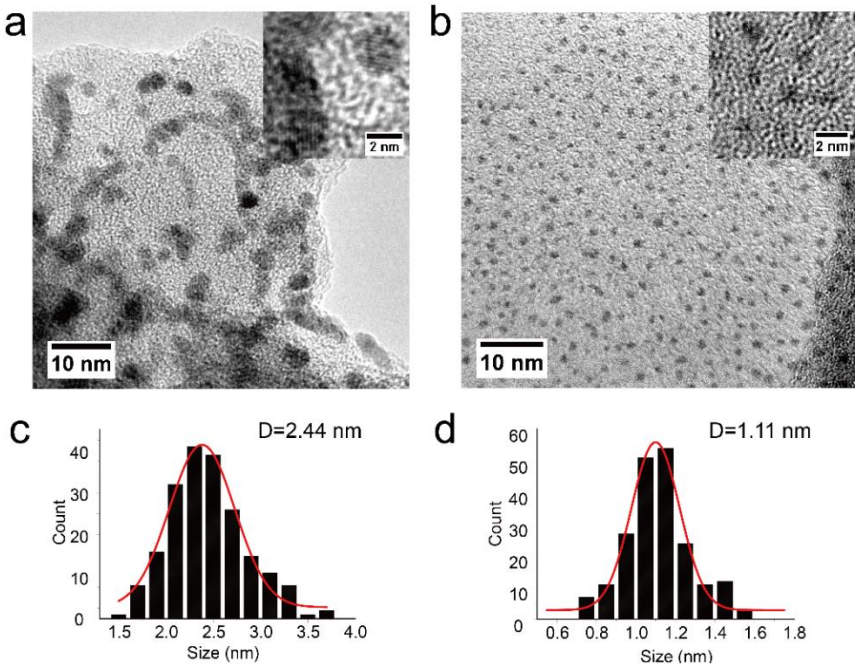

Figure S3 TEM images of (a) Pd/PANI (b) Pt/PANI, with the size distribution of (c) Pd/PANI and (d) Pt/PANI.

The size distribution of Pd and Pt NPs are shown in **Figure S3**, the mean diameter is referred as D. However, the number of Cu NPs is not sufficient, thus the mean diameter was only measured using around 30 particles.

Thus, from the enlarged TEM images (higher resolution images are shown in the inserts) shown above, the size and morphology of Cu NPs, Pd NPs and Pt NPs can be clearly identified. The Cu NPs showed sharp crystallite facets at both ends as irregular polyhedral particles, Pd NPs displayed irregular wormlike shape and Pt NPs appeared to be spherical NPs with a diameter of ~1 nm.

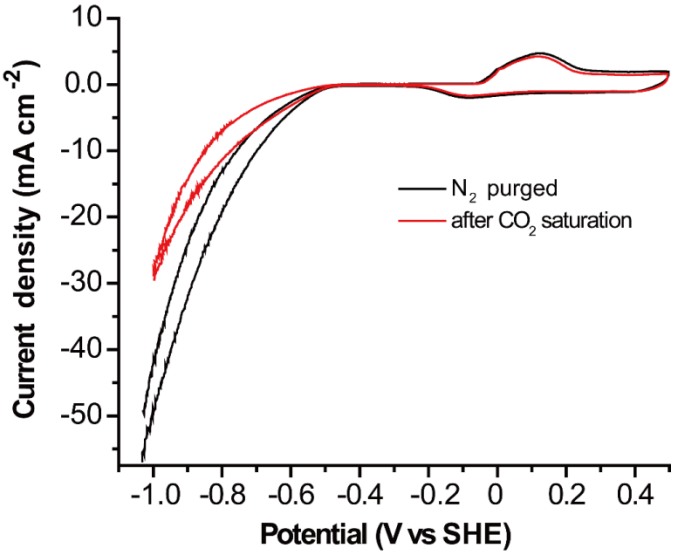

Figure S4 CV plots of Pd/PANI in 0.5 M H_2SO_4 solution purged with N_2 and saturated with CO_2, scan rate is 5 mV/s.

Figure S4 is CV plot of Pd/PANI using CO_2 saturated 0.5 M H_2SO_4 aqueous solution. The current is lower after CO_2 gas is introduced, it shows that some of the active sites are used for CO_2 reduction rather than performing hydrogen evolution reaction.

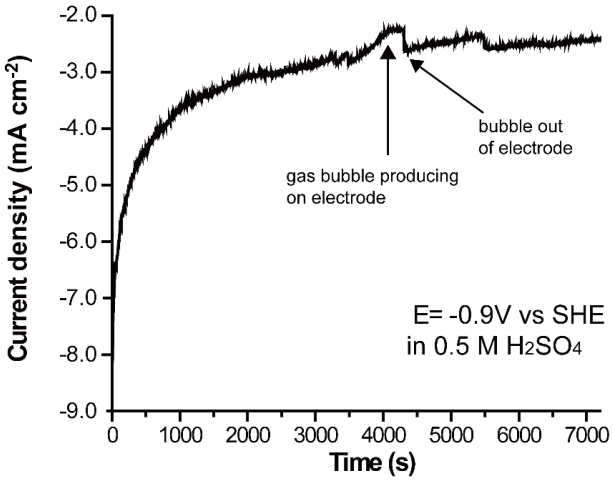

Figure S5 Chronoamperometry of Pd/PANI set at E=-0.9V (vs SHE) in 0.5 M H_2SO_4 aqueous solution saturated with CO_2 from RDE, the rotating speed was set at 800 rpm.

Figure S5 shows the current density change during CO_2 electro-reduction when applied potential is fixed at -0.9 V (the chronoamperometry studies at different voltage are quite similar). The current appears to be stable at -2.8 mA/cm^2 after 1 h according to the figure.

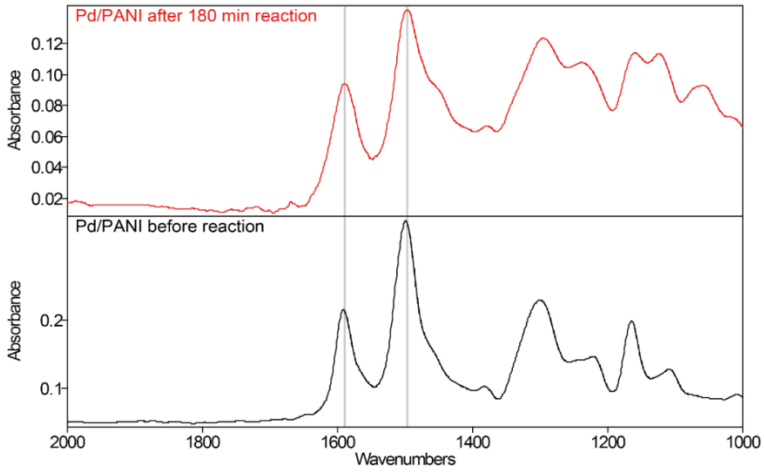

Figure S6 FTIR spectra of Pd/PANI before and after CO_2 electro-reduction.

Figure S6 shows the FTIR spectra of Pd/PANI before and after CO_2 electro-reduction. The characteristic IR bands of PANI show no significant change. Similar result was also obtained for the Cu/PANI with little change in the peak ratio at 1588 cm^{-1} and 1497 cm^{-1}. This is attributed to the fast redox change of metal-PANI.

For Pd/PANI, the total HCOOH production was 4.45 μmol/h according to the calibrated HPLC per given time. The total amount of Pd/PANI was 50 μg (10 μL of Pd/PANI solution with concentration of 5 mg PANI/mL). So the total HCOOH production per 1 g of PANI was calculated to be 89 mmol/g·h. The other data were calculated using the same way.

Current efficiency is the charge fraction used for product generation. The value was calculated based on following equation:

$$\varepsilon_{current\ efficency} = \frac{z \times n \times F}{Q}$$

Where: z is the number of electrons being used to produce a product; e.g. z=2 for CO_2 to HCOOH. n is the total mole of the product; the concentration was determined by HPLC. F is Faraday's constant; F = 96 485 C/mol. Q is the total charge been used, which can be read directly from the electrochemical station.

For example, the concentration of HCOOH is x μM, the total volume of the cell is 10 mL, then the current efficiency for HCOOH is 2x*10E-6*10*10E-3*96485/Q.

Based on equation above, the current efficiency for HCOOH and CH_3OH was calculated as below:

Table S1 HCOOH and CH_3OH production rates and total CO_2 conversion rates on Pd/PANI and Pd/PANI+Cu/PANI.

Electrode	Applied potential (vs SHE)	HCOOH production (μmol/h)	HCOOH production rate (mmol/g•h)	CH_3OH production (μmol/h)	CH_3OH production rate (mmol/g•h)	CO_2 conversion rate (mmol/ g•h)	Total charge (C)
Pd/PANI (inH_2SO_4)	-1.1	4.45	89.0	0.282	5.64	94.6	7.771
Pd/PANI + Cu/PANI (in H_2SO_4)	-0.9	1.75	35.0	0.431	8.62	43.6	6.754
Pd/PANI + Cu/PANI (in H_2SO_4)	-0.5	0.21	4.12	0.038	0.76	4.88	3.002

Table S2 Comparison of HCOOH and CH_3OH production rates of Pd/PANI & Pd/PANI+Cu/PANI with literature works

Electrode	Applied potential (vs SHE)	Current efficiency for CH_3OH (2h)	Current efficiency for HCOOH (2h)	HCOOH production (μmol/h)	CH_3OH production (μmol/h)	Current density at 30 min* (mA cm^{-2})	Ref.
Pd/PANI (in H_2SO_4)	-1.1	4.1%	22.1%	4.45	0.28	3.25	This work
Pd/PANI + Cu/PANI(in H_2SO_4)	-0.9	7.4%	10.0%	1.75	0.43	2.77	This work
Pd/PANI + Cu/PANI(in H_2SO_4)	-0.5	1.5%	2.7%	0.21	0.04	1.21	This work
Cu_2O/PANI (in MeOH/TBAP)	-0.55	N/A	7.7%	N/A	N/A	0.4	5
Pd (in $KHCO_3$)	-2.25	N/A	8.6%	N/A	N/A	N/A	6
PANI (in MeOH/$LiClO_4$)	-0.65	N/A	10.5%	25	N/A	N/A	7
Fe-PANI/PB	-1.05	0.25%	1.72%	N/A	N/A	N/A	8

*The total current density is affected by applied potential and catalyst loading.

PANI is active for CO_2 conversion to HCOOH. However, by comparing the catalytic performance of PANI and metal-PANI in Figure 1 of the main text and from the above two tables, we have found that PANI displays no activity towards HCOOH formation until the potential is lower than -0.7 V. Also, for the whole range of potentials used, there is no activity for methanol production found from PANI. Thus, we can attribute that the activity for metal-PANI to the presence of metal NPs on HCOOH production, and especially on methanol production at such potentials. In addition, in our control experiments, Pd/C or Cu/C without the inclusion of PANI did not give methanol or formic acid since the dominating reaction was the hydrogen evolution. Based on these facts, we can conclude that the interface between PANI and metal provides the active sites for CO_2 reduction however, there are obviously some degree of contributions from the individual components at negative potential lower than -0.7 V.

It should also be noted that some studies in literature have reported very high current efficiencies of above 90% which appeared to be higher than our best material: 22% for Pd/PANI considering the significant H2 evolution in our case. However, our selectivity of CO_2 reduction products (94% for HCOOH) is at least, one of the best, if not the best as compared to the reported systems in the literature.

In addition, further improvements which include metal size/shape optimizations to promote the current efficiency and selectivity are possible in this system, which is indeed a promising system for the electro-reduction of CO_2 so far.

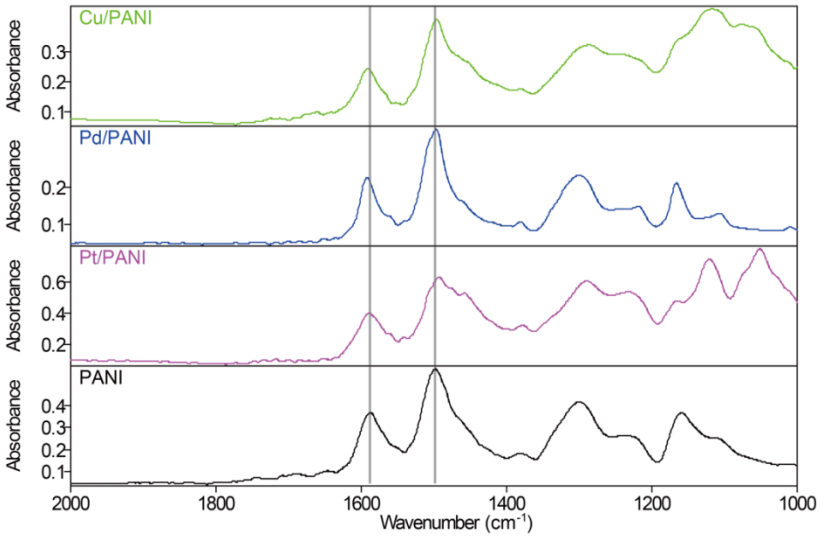

Figure S7 FTIR spectra of PANI and metal/PANI, from top to bottom: Cu/PANI, Pd/PANI, Pt/PANI and PANI.

The FTIR spectra of PANI and metal/PANI are shown in **Figure S7**. The two peaks located at 1588 cm^{-1} and 1497 cm^{-1} are characteristic of the quinoid and benzenoid structures of PANI.[4] The inclusion of metal NPs does not seem to have influence on the peak positions of the two structures. The relative peak intensity of these two peaks can indicate the oxidation state of PANI[9]. The ratio of peak intensity located at 1588 cm^{-1} and 1497 cm^{-1} appears to have increased, suggesting a degree of reduction of PANI in the presence of metal (especially Pd). However, it should be noted that the shoulder peak

(caused by charged N atoms) in the spectra of the metal/PANI materials may have affected the quantitative analysis of the above ratios, so we used Raman spectroscopy to estimate the degree of oxidation of PANI.

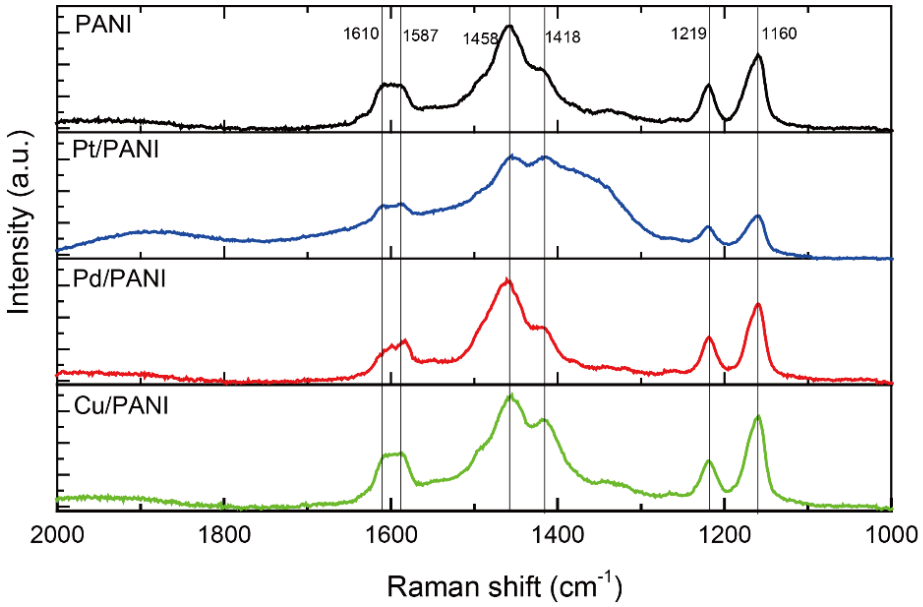

Figure S8 Raman spectra of PANI and metal/PANI, laser wavelength is 632 nm.

The Raman spectra of PANI and metal/PANI are shown in **Figure S8**. According to previous studies, the vibrational peaks at 1160 cm^{-1} and 1458 cm^{-1} are characterized with quinoid structure (oxidised unit), while peaks at 1219 cm^{-1} and 1418 cm^{-1} are associated with benzenoid structure (reduced unit).[4, 9-11] The region from 1300 cm^{-1} to 1500 cm^{-1} also includes C-N^{+}- and polaron bands[12] (probably caused by metal NPs[13]), making the deconvolution hard to solve. Thus, the oxidation degree of PANI is evaluated by the relative peak area of 1160 cm^{-1} and 1219 cm^{-1}.[14] By defining *R* to be the oxidation degree of PANI and A as the peak area, then:

$$R = A(1160cm^{-1})/A(1219cm^{-1})$$

We can calculate the relative degree of oxidation to PANI and metal/PANI, as shown in **Table S3**.

Table S3 Relative intensity analysis of Raman spectra.

Sample	*R*
PANI	2.877
PANI-Pt	3.275
PANI-Pd	2.669
PANI-Cu	2.388

Table S3 shows that the PANI is relatively more reduced with the presence of Pd and Cu, but for Pt, it becomes more oxidised presumably due to its high sensitivity towards air oxidation.

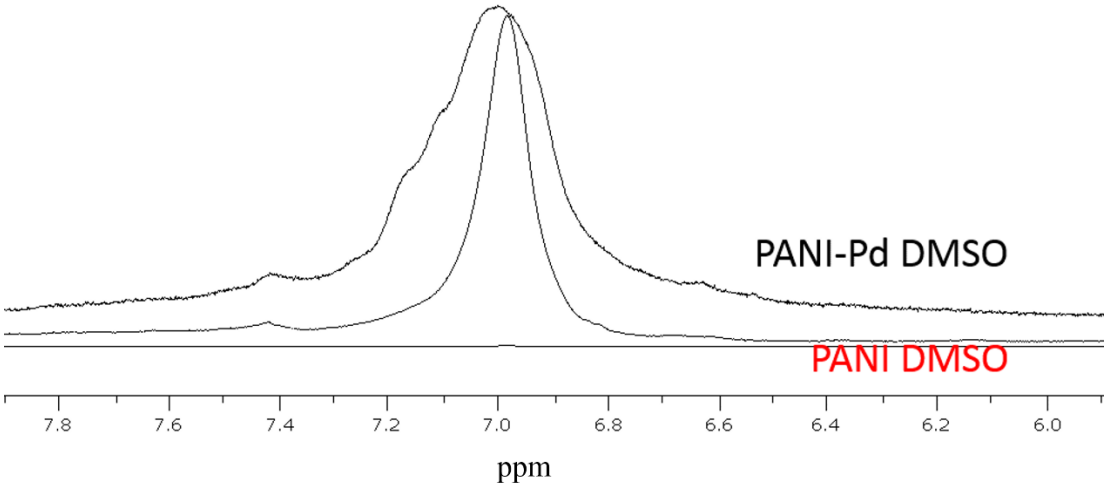

Figure S9 ^{1}H-NMR spectra of PANI and Pd/PANI, the solvent is DMSO-d6.

The ^{1}H-NMR spectra of PANI and Pd/PANI are shown in **Figure S9**. The appearance of broad shoulder peaks in Pd/PANI indicates that some chemical environments of H atoms had been altered. The increment in peak area suggests that more reduced form of PANI is found in PANI-Pd.

Thus, *without Pd atoms, there seems nothing special about electron and proton transport in PANI. However, in the presence of Pd, extensive and long-range hydrogen reduction of PANI can be taken place under the same conditions. This reduction of PANI clearly shows that Pd atoms are critical for the reduction of –N= to –NH- groups in the polymer backbone. It is envisaged that electro-reduction of* H^{+}*/electro-oxidation of* H_2 *over Pd/PANI depend on electronic and protonic transport of the material. Similarly, the formation of HCOOH from* CO_2 *requires both proton and electron, as shown in* ***Figure 1a****. Pd/PANI shows the best efficiency for HCOOH production from* CO_2 *electro-reduction in water among all the three metal catalysts studied. XPS spectra (****Figure 2b****) and NMR spectrum above (****Figure S9****) clearly show that, there is evidence of Pd-N interaction. As a result, it is evident that Pd atoms (and Pt, Cu atoms discussed in our manuscript) promote the electro-reduction of* CO_2*.*

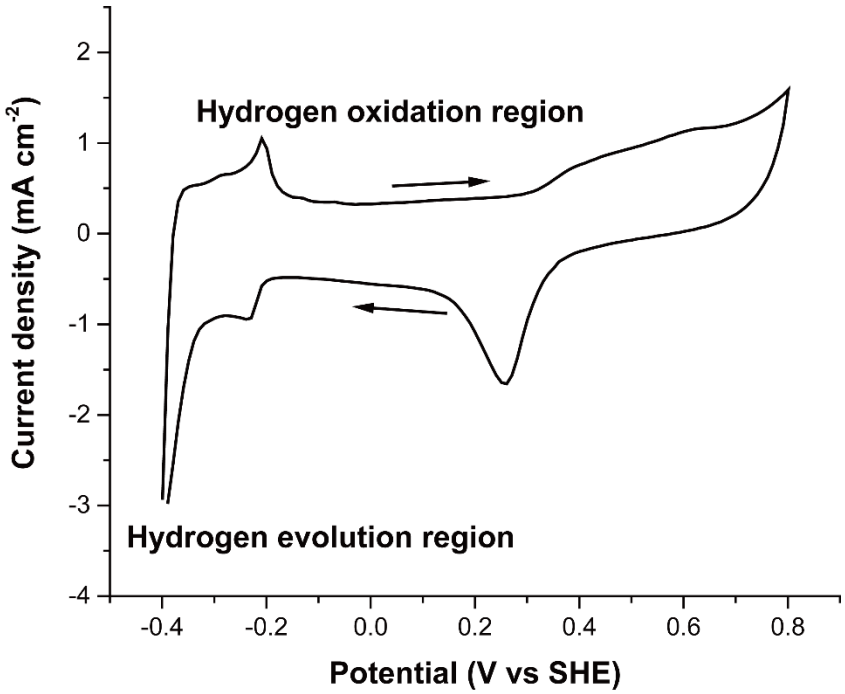

Figure S10 CV plot of Pd/C in 0.5 M H_2SO_4 aqueous solution under N_2, the scan rate is 50 mV/s. The hydrogen oxidation potential is located from -0.35 to -0.4 V.

Figure S10 shows the CV plot of Pd/C in 0.5 M H_2SO_4 solution, the normal hydrogen oxidation peak is evident from -0.35 to -0.4 V.

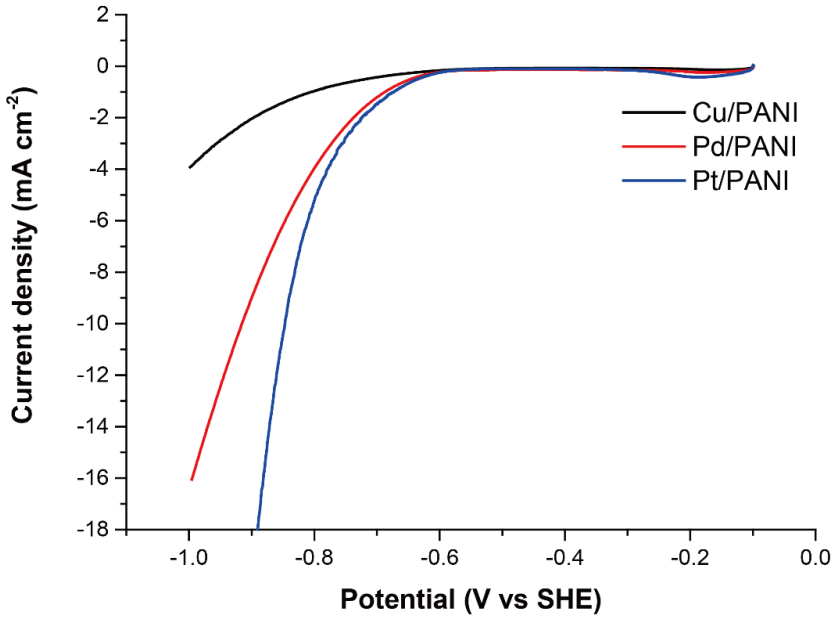

Figure S11 Hydrogen evolution reaction (HER) on Pd/PANI, Pt/PANI and Cu/PANI in 0.5 M H_2SO_4 aqueous solution, scan rate is 50 mV/s.

Figure S11 shows the HER plot of Pd/PANI, Pt/PANI and Cu/PANI catalysts. Pd/PANI and Pt/PANI have lower overpotentials for hydrogen evolution compared to Cu/PANI, but all of them have very negative onset potentials compared with Pd/C.[15]

HER generally accounted for large fraction of cathodic current if metal is placed in acidic conditions within the negative potential range. Indeed, from our control experiments, Pd/C or Cu/C without the inclusion of PANI did not give methanol or formic acid at all but the dominating reaction was the hydrogen evolution at below -0.4V (Fig. S10, see also Table 2 of Pd ($KHCO_3$) with the lowest activity for formic acid production). However, the conductivity of PANI is lower when it is in reduced form in acidic conditions, thus causing higher over-potential for HER (no H_2 production at -0.35 to -0.4 V), as shown in the above Figure S11. By using this unusual interface, in-situ generated Metal-H for hydrogenation of CO_2 other than H, H combination producing H_2 can be achieved.

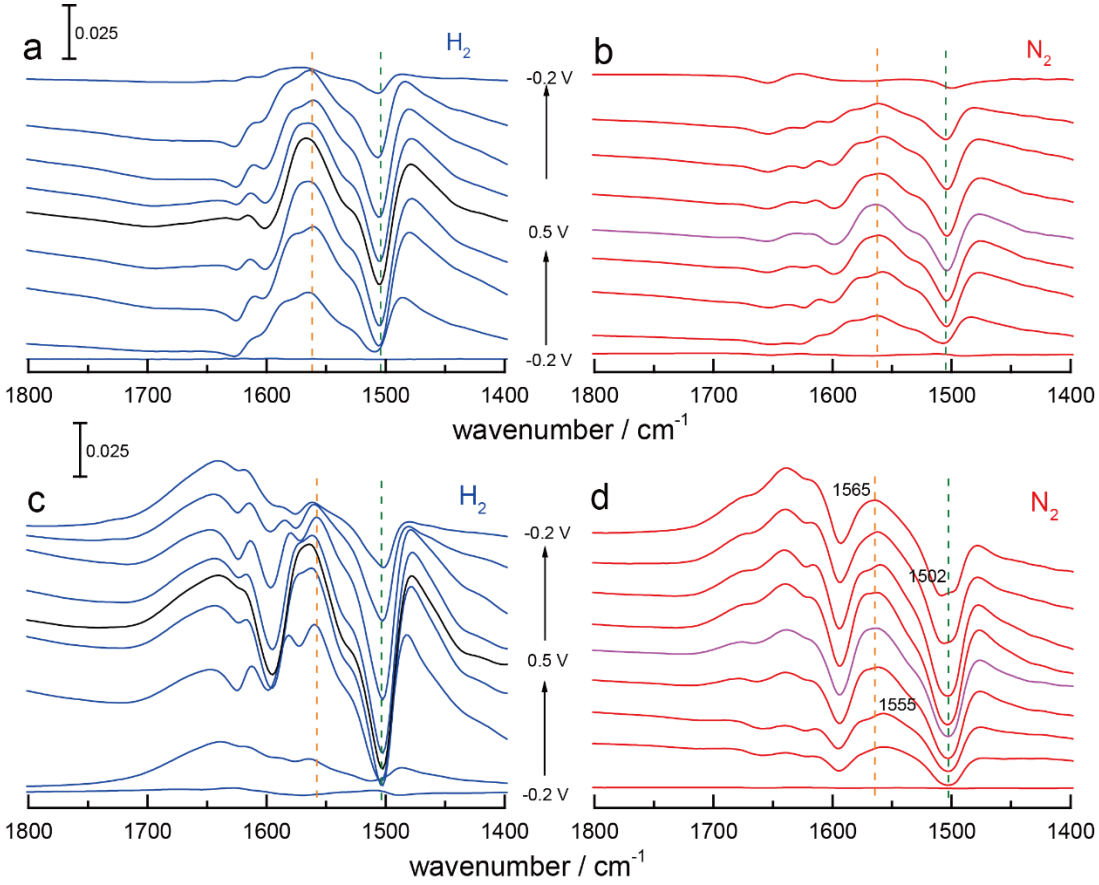

Figure S12 *In situ* electrochemical ATR-IR spectra of (a) Pd/PANI under H_2, (b) Pd/PANI under N_2, (c) PANI under H_2 and (d) PANI under N_2.

Figure S12 shows the *in situ* electrochemical ATR-IR spectra of Pd/PANI and PANI under H_2 and N_2 atmospheres. Comparing Pd/PANI and PANI under H_2 (**Figure S12a** and **Figure S12c**), the peak intensity of C=C (PANI: 1505 cm^{-1}, Pd/PANI: 1501 cm^{-1}) decreases while that of C=N (PANI: 1558 cm^{-1}, Pd/PANI: 1565 cm^{-1}) rising during oxidation (from -0.2 V to 0.5 V), indicative of decreasing

benzenoid and increasing quinoid structures, and vice versa. The peak intensity of N-H deformation (Pd/PANI: 1601 cm^{-1}, PANI: 1595 cm^{-1}) also decreases during the oxidation. The new peak (Pd/PANI: 1611 cm^{-1}, PANI: 1614 cm^{-1}) is considered to be a characteristic vibrational band of PB and can be assigned to a –C=C-C=N- asymmetrical vibrational mode. As to Pd/PANI and PANI under N_2 (**Figure S12b** and **Figure S12d**), the trend of C=C and C=N structures are similar with samples under H_2. But the absorption of N-H deformation (Pd/PANI: 1602 cm^{-1}, PANI: 1595 cm^{-1}) is smaller in Pd/PANI than in PANI, suggesting that Pd can stabilize the N-H structure and reduce PANI.

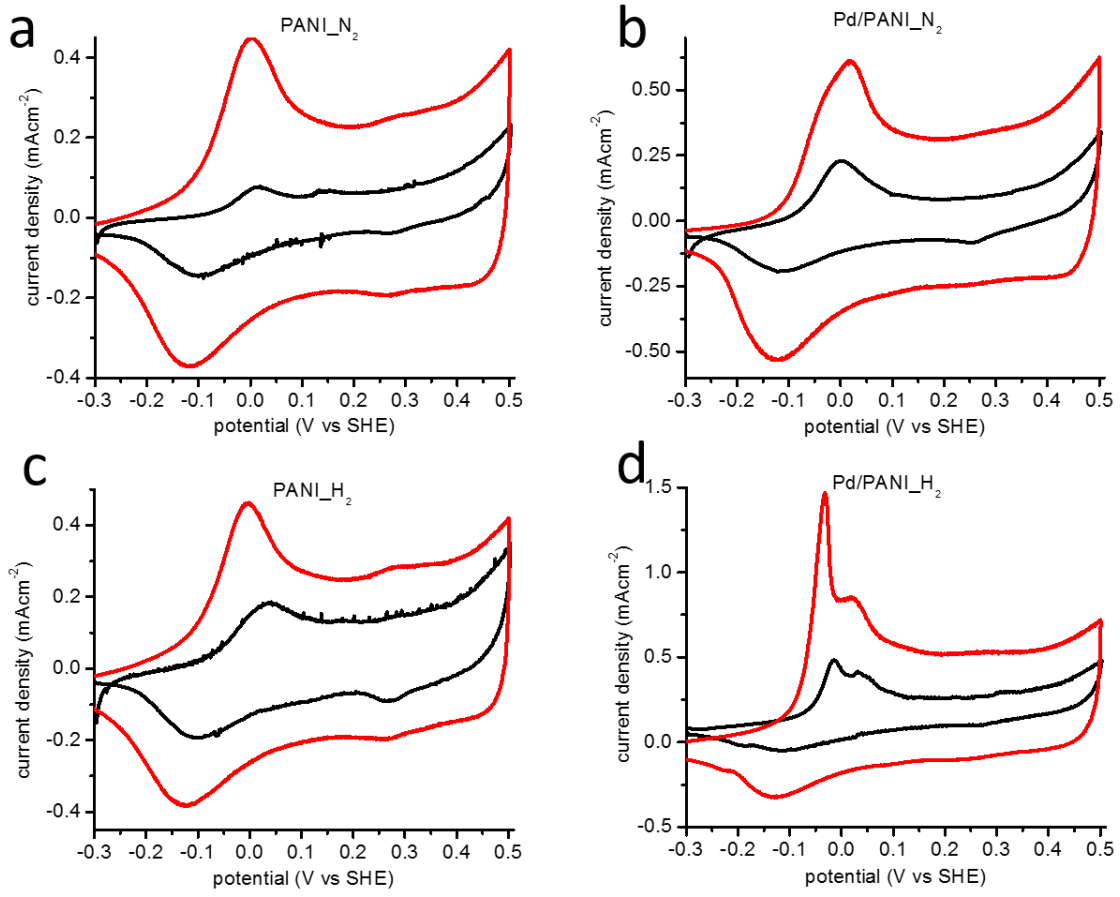

Figure S13 CV plots of Pd/PANI and PANI under H_2 and N_2 atmosphere in 0.5 M H_2SO_4 aqueous solution. Solid black line is for *in situ* ATR-IR experiment and solid red line is from RDE experiment.

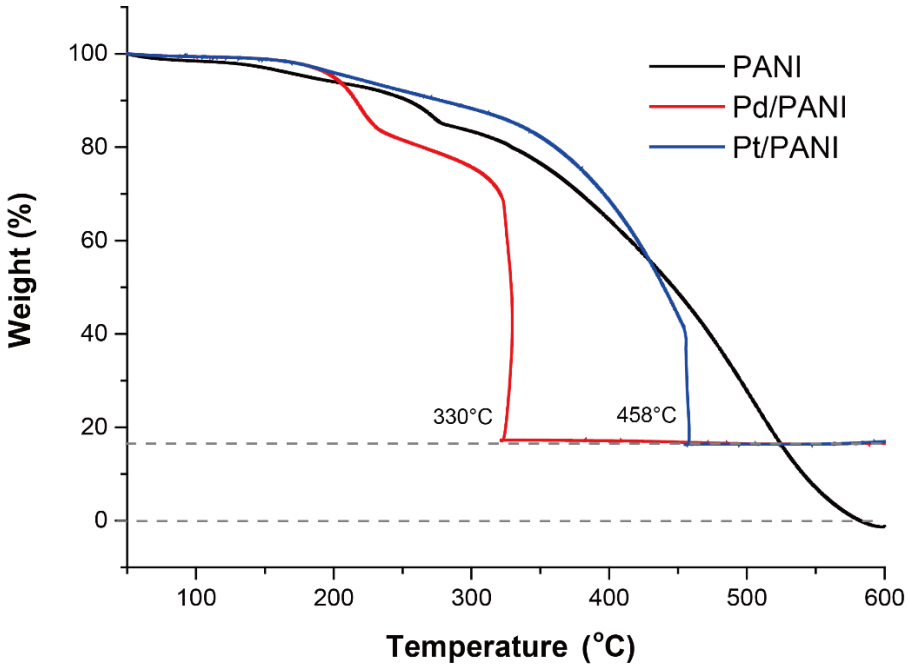

Figure S14 TGA plots of PANI, Pd/PANI and Pt/PANI in air, heating rate is 5 °C/min.

Figure S14 shows the TGA plots of PANI and metal/PANI. By introducing metal NPs PANI becomes more unstable against combustion. [16]

Quantitative treatment of TPD:

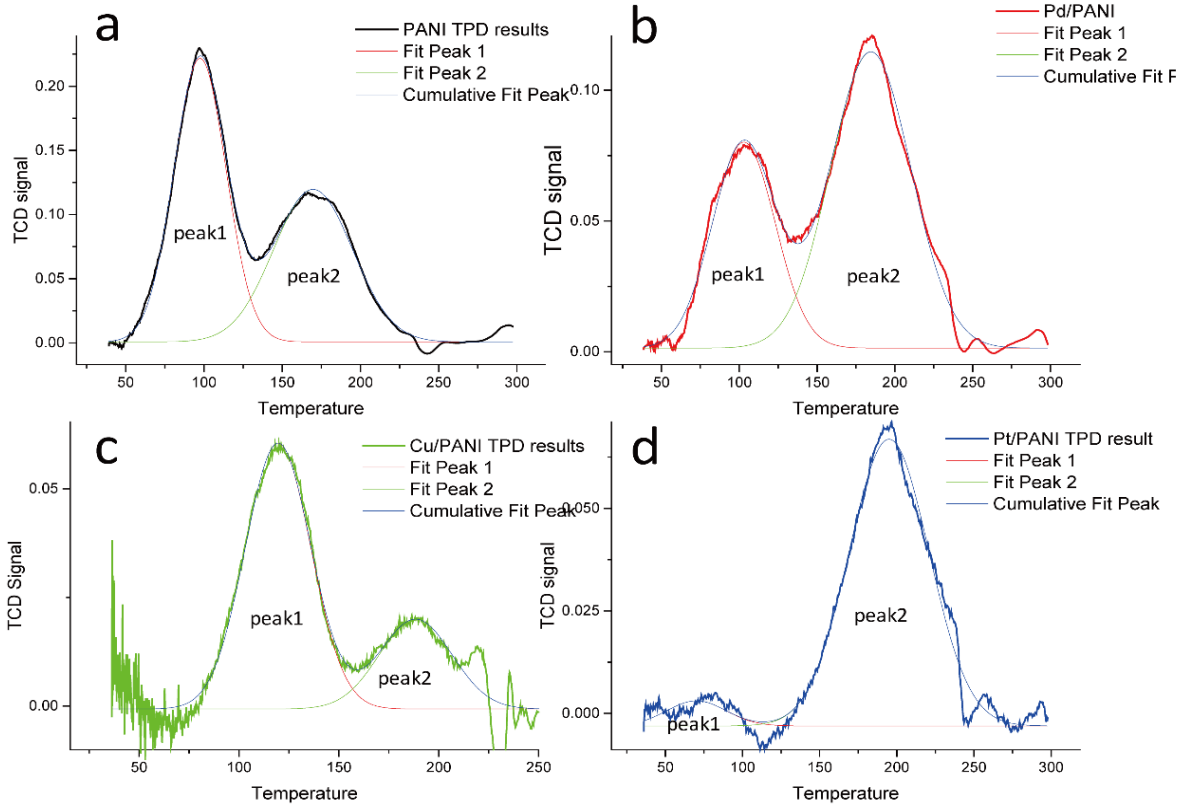

Figure S15 TPD fitting results of (a) PANI, (b) Pd/PANI, (c) Cu/PANI and (d) Pt/PANI.

30 mg of samples were used for CO_2 TPD test. The TPD data were fitted as shown in **Figure S15**, and summarized in **Table S4**.

Table S4 CO_2 TPD results of PANI and metal/PANI samples.

Sample	Peak 1 position (°C)	Peak 1 area*	Peak 1 CO_2 uptake (mmol/g PANI)	Peak 2 position (°C)	Peak 2 Area*	Peak 2 CO_2 uptake (mmol/g PANI)	Total CO_2 uptake** (mmol/g PANI)
PANI	96.6	9.25	0.75	167.4	7.52	0.61	1.36
Pd/PANI	102.9	4.92	0.40	184.5	9.05	0.73	1.13
Pt/PANI	70.9	0.42	0.03	195.0	6.54	0.53	0.56
Cu/PANI	125.7	2.87	0.23	188.4	1.07	0.09	0.32

*The peak areas of CO_2 TPD on Metal/PANI samples are normalized to PANI mass and 1 g of PANI contains 10.97 mmol N atoms.
**Total CO_2 uptake is calculated by peak 1 and peak 2 areas.

According to our calibration of CO_2:

$$CO_2(mmol) = 0.00243 * Peak\ area - 3.12 * 10^{-5}$$

Fitting the total peak area gave the total CO_2 adsorption for 30 mg of samples. The CO_2 uptake values (mmol/g PANI) were then calculated by normalizing the amount of PANI to 1 g (1g Pd/PANI contains 0.811 g PANI, 1 g Pt/PANI contains 0.700 g PANI and 1 g Cu/PANI contains 0.879 g PANI).

All the products were analysed using both GC and HPLC results. The typical HPLC result of products of CO_2 electrochemical reduction at -0.7 V (vs SCE) using Pd/PANI as catalyst, is shown in Figure S15.

It is unfortunately that we were unable to compare the CV results with the above CO_2 desorption studies with confidence since it was rather tricky to sort it out even with the help of in-situ IR. We did not find any carbonate anion related signals in all of the methods. Notably, Figure 4 in the main manuscript showed the comparison of PANI and metal/PANI samples before and after CO_2 treatment. Carbonate anion is hard to see from TPD considering the principle of the method is heating up and forcing desorption. FTIR shows only one peak around 1656 cm^{-1}, agreeing quite well with the peak of O-C-O asymmetric stretch (Zheng, W.; Qu, J.; Hong, X.; Tedsree, K.; Tsang, S. C. E. ChemCatChem 2015, 7 (23), 3826.). The carbonate, if exist, should also show a peak around 1790-1760 cm^{-1}(Smith, B. C. Infrared spectral interpretation: a systematic approach. 1999; CRC Press: New York.), but no prominent peak was found probably due to high background at that range.

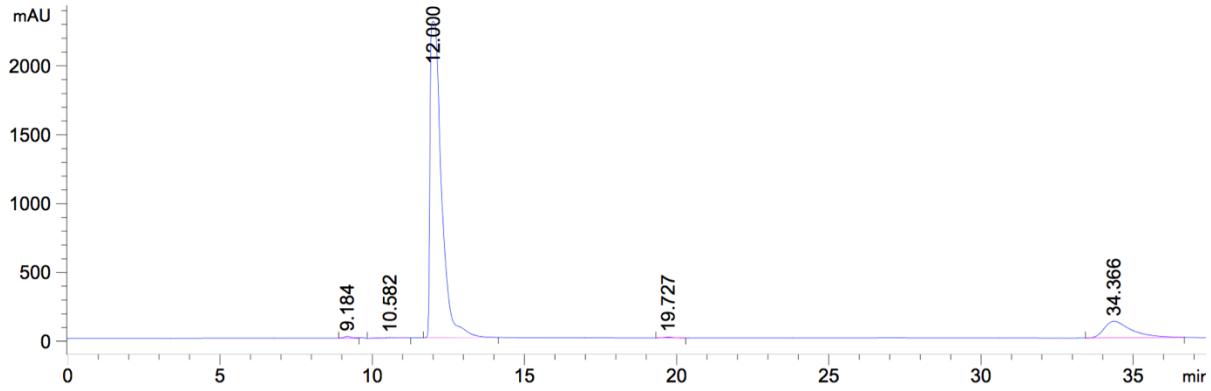

Figure S16 HPLC spectrum of products of CO_2 electro-reduction at -0.7 V (vs SCE) using Pd/PANI as catalyst.

As shown in **Figure S16**, the main products were formic acid (t=12.000 min) and methanol (t=34.366 min). The peaks at 9.184 min and 10.582 min were due to the concentration changes of mobile phase.

The peak at 19.727 min could be assigned to another product, but the peak area is too small comparing to that of formic acid and methanol.

Reference and notes:

1 J. Huang, R. B. Kaner, *Angew. Chem., Int. Ed.* 2004, **43**, 5817.

2 R. Hidalgo, P. A. Ash, A. J. Healy, K.A. Vincent, *Angew. Chem., Int. Ed.*, 2015, **54**, 7110.

3 A. J. Healy, P. A. Ash, O. Lenz, K. A. Vincent, *Phys. Chem. Chem. Phys.*, 2013,**15**, 7055.

4 E. T. Kang, K. G. Neoh, K. L. Tan, *Prog. Polym. Sci.* 1998, **23**, 277.

5 A. N. Grace, S. Y. Choi, M. Vinoba, M. Bhagiyalakshmi, D. H. Chu, Y. Yoon, S. C. Nam, S. K. Jeong, *Appl. Energy* 2014, **120**, 85.

6 M. Azuma, K. Hashimoto, M. Watanabe, T. Sakata, *J. Electroanal. Chem*. 1990, **294**, 299.

7 F. Köleli, T. Röpke, C. H. Hamann, *Synth. Met.* 2004, **140**, 65.

8 K. Ogura, *J. Electrochem. Soc*. 1995, **142**, 4026.

9 R. K. Pandey, V. Lakshminarayanan, *J. Phys. Chem. C* 2009, **113**, 21596.

10 A. Gruger, A. Novak, A. Régis, P. Colomban, *J. Mol. Struct.* 1994, **328**, 153.

11 A. Drelinkiewicz, M. Hasik, M. Choczynski, *Mater. Res. Bull.* 1998, **33**, 739.

12 M. C. Bernard, A. Hugot-Le Goff, *Synth. Met.* 1997, **85**, 1145.

13 R. J. Tseng, C. O. Baker, B. Shedd, J. Huang, R. B. Kaner, J. Ouyang, Y. Yang, *Appl. Phys. Lett.* 2007, **90**, 1.

14 N. S. Sariciftci, M. Bartonek, H. Kuzmany, H. Neugebauer, A. Neckel, *Synth. Met.* 1989, **29**, 193.

15 A. Nirmala Grace, K. Pandian, *Electrochem. Commun.* 2006, **8**, 1340.

16 S. Harish, J. Mathiyarasu, K. L. N. Phani, V. Yegnaraman, *Catal. Letters* 2009, **128**, 197.